

Report

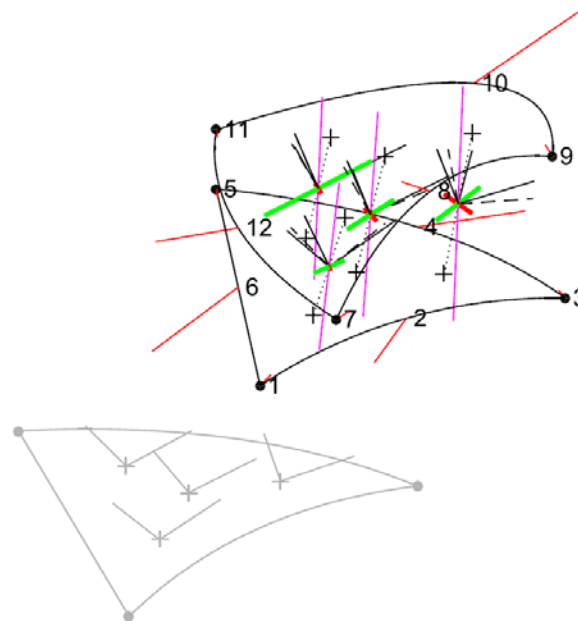
Modeling hydrogen transport and hydrogen-induced embrittlement

Manual for DIFEL and CZE elements

Author(s)

Philippe Mainçon

-



Report

Modeling hydrogen transport and hydrogen-induced embrittlement

Manual for DIFEL and CZE elements

KEYWORDS:

hydrogen
embrittlement
modelling
cohesive zone element
hydrogen diffusion

VERSION
V1

DATE
2020-11-19

AUTHOR(S)
Philippe Mainçon
-

CLIENT(S)
Multiclient KPN

CLIENT'S REF.
-

PROJECT NO.
102017484-6

NUMBER OF PAGES/APPENDICES:
4 + Appendices

ABSTRACT

This document provides the theory manual and user manual for two finite elements for the modeling of hydrogen-induced embrittlement of metallic materials. The cohesive zone element (CZE) allows to simulate the creation of new surfaces and the corresponding absorption of energy. The absorption of energy is made a function of the hydrogen concentration. The volume element (DIFEL) accounts for mechanical deformation, the transport of hydrogen, and the kinetics of trapping and untrapping.

PREPARED BY
Philippe Mainçon

SIGNATURE


Philippe Mainçon (Nov 30, 2020 13:18 GMT+1)

CHECKED BY
Vigdis Olden

SIGNATURE



APPROVED BY
Magnus Eriksson

SIGNATURE



REPORT NO.
2020:01275

ISBN
978-82-14-06445-2

CLASSIFICATION
Unrestricted

CLASSIFICATION THIS PAGE
Unrestricted

Document history

VERSION	DATE	VERSION DESCRIPTION
V1	2020-11-23	Initial version

Contents

1	Introduction	5
2	CZE: Cohesive zone element	5
2.1	Features	5
2.1.0.1	Solute diffusion	5
2.1.0.2	Multiple elements	6
2.1.0.3	Tangential strains	6
2.1.0.4	Research-oriented	6
2.2	Formulation	7
2.2.1	Reference systems	7
2.2.2	Shape functions	8
2.2.3	Solute concentration	8
2.2.4	Gap	8
2.2.5	Strain	9
2.2.6	Nodal forces	9
2.2.7	Nodal flow	10
2.3	CZE/ABAQUS interface	11
2.3.1	Node and degree of freedom numbering	11
2.3.2	Limitations	11
2.4	TSL/CZE interface	13
3	DIFEL: element for diffusion and capture	13
3.1	Mechanics	13
3.1.1	Hypotheses	13
3.1.2	Equations	14
3.1.3	Formulation	14
3.1.3.1	Deformation gradient	14
3.1.3.2	Isoparametric element	15
3.1.3.3	Mixed element	15
3.1.4	Plasticity	16
3.2	Heat diffusion	17
3.3	Mass diffusion and trapping	17

3.3.1	Trapping	17
3.3.1.1	Working with kinetics	17
3.3.1.2	Chemical reaction network	18
3.3.1.3	State transition reactions	19
3.3.1.4	“Many lattice site” approximation	19
3.3.1.5	Law of mass action	20
3.3.1.6	General purpose model	20
3.3.1.7	Improving convergence	20
3.3.2	Diffusion and conservation	23
3.3.3	Weak form	23
4	User manual	24
A	Sample *.inp file	27
	References	32

1 Introduction

This document provides the theory manual and user manual for two finite elements for the modeling of hydrogen-induced embrittlement of metallic materials. The cohesive zone element (CZE) allows to simulate the creation of new surfaces and the corresponding absorption of energy. The absorption of energy is made a function of the hydrogen concentration. The volume element (DIFEL) accounts for mechanical deformation, the transport of hydrogen, and the kinetics of trapping and untrapping.

Although plastic deformation and hydrogen diffusion driven by triaxial pressure have been implemented, these have not been tested and the current input format does not support them. Heat diffusion has not been tested either.

Both elements are implemented as “user-defined elements” (UEL) for ABAQUS. This has proven to be an extremely costly strategy because ABAQUS’s support for UELs is actually extremely poor. As a consequence, the version of DIFEL and CZE documented here is the last that will be implemented for ABAQUS, and further development will have to wait for a re-implementation which is being planned at the time of writing.

2 CZE: Cohesive zone element

2.1 Features

The present document is intended both as a theory manual and a developers manual for CZE. `.f90`, `TSL.f90` and ancillary code. This code was written to provide flexibility in the modeling of the effect of solutes (in particular hydrogen) on the fracture of metallic material, using cohesive-zone modeling.

CZ models are common, and SINTEF actually disposed CZ code for ABAQUS prior to the development reported here. The present code provides several capabilities:

2.1.0.1 Solute diffusion

Element nodes can have one or several degree of freedoms for the concentration of solutes (hydrogen and so forth). The CZ element can handle the diffusion of hydrogen across it, the effect of separation on the permeability, and the effect of solute concentration on the traction separation law.

Isoparametric formulation

The code uses an isoparametric formulation to provide maximum flexibility in meshing. Local reference systems are introduced at each Gauss point, so that curved elements are properly handled.

2.1.0.2 Multiple elements

The present code handles both 3D and 2D analyses and provides isoparametric transforms of triangle, square and segment. New elements (with higher number of nodes and/or higher numbers of Gauss points) can easily be added. “Over-integration”, with higher numbers of Gauss point can be a strategy to handle the strong non-linearity of the traction separation law.

An element type is defined by just a few lines of code, that specify the layout of nodes, and degrees of shape functions. For example, the subroutine `UEL` in `ue1.f90` contains:

```

1 case (2)    !'CZE_RECT8H4
2 ! cohesize zone, rectangle, 8 nodes, solute, 4 nodes
3     ga      = Legendre(4)
4     quad    = ga*ga
5     call CZelement(coords,u,v,a,alfa,rhs(1:ndofel,1),amat,
6         svars,props,jprops,quad,jtype,jelem,kstep,kinc,&
7     xterm   = reshape
8         ([0,1,0,2,1,0,2,1,0,0,1,0,1,2,1,2],[8,2]),&
9     sterm   = reshape([0,1,0,1,0,0,1,1],[4,2]),&
10    znod    = reshape([-1.0_dp, 0.0_dp, 1.0_dp, 1.0_dp, 1.0
11    _dp, 0.0_dp,-1.0_dp,-1.0_dp,&
12    -1.0_dp,-1.0_dp,-1.0_dp, 0.0_dp, 1.0_dp, 1.0_dp, 1.0_dp, 0.0
13    _dp],[8,2]),&
14    sznod   = [1,3,5,7],&
15    scala   = scalefac)

```

2.1.0.3 Tangential strains

While the CZ element has initial zero thickness, it actually represents a process zone with possibly finite stiffness. In particular, in the case of ductile failure, tangential stresses promote void growth over a brittle mechanism, and conversely, void growth induces a local relaxation of tangential stresses. This may be a mechanism of the influence of “constraint” on the fracture toughness.

The present formulation handles this by providing the TSL (traction separation law) with tangential strains, and accepting tangential “stresses” (actually, multiplied by the thickness of the process zone) in return.

2.1.0.4 Research-oriented

The present implementation focuses on flexibility and maintainability, not on performance:

- Expansion of shape function arrays serves code readability, not performance.

- Operations that could be done at compile time, or at the start of the analysis, are repeated at each iteration.
- The element “stiffness” matrix is computed from the element “forces” by finite differences. This simplifies the code for the element, and not least, that of traction separation laws.
- Isoparametric formulation is used to cope with a wide range of meshes. This is used for all element types, although triangular elements do not gain anything from isoparametric formulation.

Hopefully, the performance loss thus incurred is insignificant, as the bulk of CPU time should be consumed by the volume elements in the model, and/or the solution of the system of equations for the whole model.

2.2 Formulation

2.2.1 Reference systems

The present family of elements uses isoparametric formulations. Because of the necessity to distinguish components of various tensors that are normal and tangential to the element, it is necessary to introduce reference systems that are not present, at least in typical volume elements.

These reference systems are described in this section.

In the code and this document, x -coordinates refer to the “global”, “canonical” or “Eulerian” orthonormal reference system. This is for example the reference system in which ABAQUS expresses node coordinates or displacements. The base has n_x dimensions, 2 in membrane analysis, 3 in volume analysis.

Isoparametric elements are classically described in a “reference” configuration. For example, in that reference configuration, all triangular elements have vertices with coordinates $(0,0)$, $(1,0)$ and $(0,1)$. All “square” elements have vertices with coordinates $(-1,-1)$, $(1,-1)$, $(1,1)$ and $(-1,1)$. These coordinates, often described as ζ -coordinates in the literature, are referred to as z -coordinates here and in the code. There are $n_z = n_x - 1$ such coordinates. The position of nodes and Gauss integration points is expressed in this reference system. At each Gauss point, a base is defined, which vectors are the partial derivative of a point with respect to each z -coordinate.

The “initial” configuration is the as meshed geometry. The convected of the z -base by the transformation from the reference to the initial configuration is a general base. It is orthonormalised using Gram-Charlier: the convected of \bar{z}_1 is normalized, yielding \bar{y}_1^0 , and the convected of \bar{z}_2 is made orthogonal to \bar{y}_1^0 and normalized, yielding \bar{y}_2^0 . We then introduce $\bar{y}_3^0 = \bar{y}_1^0 \times \bar{y}_2^0 / |\bar{y}_1^0 \times \bar{y}_2^0|$, completing the “ y^0 -base”. This cross product is necessary because, while one could introduce a third vector in the z -base, there is no way convect it with the deformation of the element, since the element’s displacement field is only defined with a 2D surface.

At any time \mathbf{t} , we can introduce the convected of the above base by the transformation from initial to instantaneous configuration, yielding $\bar{\mathbf{y}}_1^{\mathbf{t}}$ and $\bar{\mathbf{y}}_2^{\mathbf{t}}$. We then introduce $\bar{\mathbf{y}}_3^{\mathbf{t}} = \bar{\mathbf{y}}_1^{\mathbf{t}} \times \bar{\mathbf{y}}_2^{\mathbf{t}} / |\bar{\mathbf{y}}_1^{\mathbf{t}} \times \bar{\mathbf{y}}_2^{\mathbf{t}}|$. This defines the “ \mathbf{y} -base”, which coordinates in the \mathbf{x} base are found in the code as \mathbf{x}_y . The \mathbf{y} -base is not orthonormal, so the coordinates \mathbf{y}_x of its dual base appear in the computation.

The stress to be returned by the traction separation law is the 2 Piola–Kirchhoff tensor, expressed in the \mathbf{y}^0 -base (which is its own dual). The traction to be returned by the traction separation is the traction per unit of *initial* surface (or the traction per unit of instantaneous surface, multiplied by the Jacobian determinant), to be expressed in the dual of the \mathbf{y} -base.

2.2.2 Shape functions

We consider the array \mathbf{A} of size $\mathbf{nznod} \times \mathbf{ngp}$, which contains the value of the displacement at a Gauss point, corresponding the displacement of a node in a face. Similarly, we consider the array \mathbf{B} of size $\mathbf{nznod} \times \mathbf{nz} \times \mathbf{ngp}$ containing the values at the Gauss points of the gradients of the derivatives of the displacement, corresponding to a nodal displacement. These are the classical shape functions of membrane elements.

From these, the following arrays are constructed:

\mathbf{A}_δ which to the displacement in each of \mathbf{nx} directions, of each node of each face, associates the coordinates of the gap vector at each Gauss point, expressed in the global \mathbf{x} -coordinate system.

\mathbf{A}_s which to the concentration of each solute, at each node of each face, associates the concentration of each solute at each Gauss point, averaged over the two faces.

\mathbf{B}_z which to the displacement in each of \mathbf{nx} directions, of each node of each face, associates the gradient with respect to \mathbf{z} -coordinates of displacement expressed in the global \mathbf{x} -coordinate system at each Gauss point, averaged over the two faces.

\mathbf{B}_y is the same as \mathbf{B}_z , but the gradients are with respect to the \mathbf{y} -coordinates.

2.2.3 Solute concentration

For each solute, concentration is a scalar, and for each phase, its interpolation from nodal values is done in the usual fashion. The concentration at a Gauss point, transmitted to the TSL is the mean of the concentrations at each face.

2.2.4 Gap

In volume elements, the coordinates of a point within the element are found by multiplying the vector of nodal coordinates by the shape functions. In the present implementation, this is done for each face, and the results are subtracted to yield the gap. More specifically, the shape function \mathbf{Ns} is constructed to directly yield the

difference. This gives the coordinates of the gap in the \mathbf{x} -base. This is re-expressed in the \mathbf{y}^t -base by projection on its dual base (by solving $\mathbf{gap} = \mathbf{LU} \mathbf{solve}(\mathbf{x}_y, \mathbf{gap})$).

$$\bar{\delta} = \delta_i^x \bar{x}_i \quad (2.1)$$

$$= \delta_i^y \bar{y}_i^t \quad (2.2)$$

As a consequence, (in a 3D analysis), the two first coordinates of the gap are tangential values in material-orthogonal directions. The third component is the opening in the instantaneous-normal direction. Positive values refer to an opening, negative to interpenetration of the faces.

2.2.5 Strain

Green-Lagrange strain and their computation in a FEA setting are well documented in the literature. In the present setting, there is a small deviation from the canonical theory because only the strain within the plane tangent to the element are computed: The deformation gradient is $\bar{\mathbf{F}} = \bar{\mathbf{y}}_i^t \underline{\mathbf{y}}_i^0$ contains the coordinates $\bar{\mathbf{y}}_1^t$ and $\bar{\mathbf{y}}_2^t$ in the \mathbf{x} -base, and is of size $\mathbf{nx} \times \mathbf{nz}$. As a result

$$\bar{\bar{\boldsymbol{\varepsilon}}} = \frac{1}{2} (\bar{\mathbf{F}}^T \cdot \bar{\mathbf{F}} - \bar{\mathbf{I}}) \quad (2.3)$$

$$= \frac{1}{2} (\underline{\mathbf{y}}_i^0 \bar{\mathbf{y}}_i^t \cdot \bar{\mathbf{y}}_j^t \underline{\mathbf{y}}_j^0 - \underline{\mathbf{y}}_i^0 \bar{\mathbf{y}}_i^0 \cdot \bar{\mathbf{y}}_j^0 \underline{\mathbf{y}}_j^0) \quad (2.4)$$

$$= \frac{1}{2} (\bar{\mathbf{y}}_i^t \cdot \bar{\mathbf{y}}_j^t - \bar{\mathbf{y}}_i^0 \cdot \bar{\mathbf{y}}_j^0) \underline{\mathbf{y}}_i^0 \underline{\mathbf{y}}_j^0 \quad (2.5)$$

$$= \frac{1}{2} (\bar{\mathbf{y}}_i^t \cdot \bar{\mathbf{y}}_j^t - \delta_{ij}) \underline{\mathbf{y}}_i^0 \underline{\mathbf{y}}_j^0 \quad (2.6)$$

$$= \varepsilon_{ij}^y \underline{\mathbf{y}}_i^0 \underline{\mathbf{y}}_j^0 \quad (2.7)$$

is of size $\mathbf{nz} \times \mathbf{nz}$: it is a material strain expressed in terms of coordinates in the orthonormal base \mathbf{y}^0 (built by Gram-Charlier orthonormalisation).

2.2.6 Nodal forces

The work in the element is equal to

$$\mathcal{W} = \int_{V_{\mathbf{y}^0}} \mathcal{W} dV_{\mathbf{y}^0} \quad (2.8)$$

$$= \int_{V_{\mathbf{y}^0}} \mathcal{W} J dV_z \quad (2.9)$$

\mathcal{W} is a function of $\bar{\bar{\epsilon}}_y$, $\bar{\delta}$ and s_i . The two firsts are functions of the nodal position, and by definition the nodal forces are

$$R^i = \frac{\partial \mathcal{W}}{\partial X_i} \quad (2.10)$$

$$= \int_{V_{y^0}} \frac{\partial}{\partial X_i} (WJ) dV_z \quad (2.11)$$

$$= \int_{V_{y^0}} \left(\frac{\partial W}{\partial X_i} J + W \frac{\partial J}{\partial X_i} \right) dV_z \quad (2.12)$$

$$\approx \int_{V_{y^0}} \frac{\partial W}{\partial X_i} J dV_z \quad (2.13)$$

$$= \int_{V_{y^0}} \left(\frac{\partial W}{\partial \delta_j^y} \frac{\partial \delta_j^y}{\partial X_i} + \frac{\partial W}{\partial \epsilon_{jk}^y} \frac{\partial \epsilon_{jk}^y}{\partial X_i} \right) J dV_z \quad (2.14)$$

$$= \int_{V_{y^0}} \left(t_j^y \frac{\partial \delta_k^x}{\partial X_i} \frac{\partial \delta_j^y}{\partial \delta_k^x} + \sigma_{jk}^y \frac{\partial \epsilon_{jk}^y}{\partial X_i} \right) J dV_z \quad (2.15)$$

$$= \int_{V_{y^0}} \left(t_j^y N_{ik} F_{kj} + \sigma_{jk}^y B_{ilj} F_{lk} \right) dV_{y^0} \quad (2.16)$$

$$R = \int_{V_{y^0}} (N \cdot F \cdot t^y + B : (F \cdot \sigma^y)) dV_{y^0} \quad (2.17)$$

A comment: in the term in t_j^y the sum over j spans \mathbf{nx} , while in the term in σ_{kj}^y , the sum over k spans \mathbf{nz} .

By construction, σ^y are the \mathbf{y} -coordinates of the 2nd Piola-Kirchhoff stress tensor: both surface direction, surface measures and tractions relate to the initial configuration and are expressed in \mathbf{y} -coordinates. Similarly, t^y are the \mathbf{y} -coordinates of tractions related to the initial configuration. They are per unit of initial surface.

2.2.7 Nodal flow

Similarly, the nodal flow is, by definition, the dual of the work with respect to the nodal concentrations:

$$Q^i = \frac{\partial \mathcal{W}}{\partial S_i} \quad (2.18)$$

$$= \int_{V_{y^0}} \frac{\partial}{\partial S_i} (\mathcal{W}J) dV_z \quad (2.19)$$

$$= \int_{V_{y^0}} \frac{\partial \mathcal{W}}{\partial S_i} J dV_z \quad (2.20)$$

$$= \int_{V_{y^0}} \frac{\partial \mathcal{W}}{\partial s_j} \frac{\partial s_j}{\partial S_i} dV_{y^0} \quad (2.21)$$

$$= \int_{V_{y^0}} q_j M_{ij} dV_{y^0} \quad (2.22)$$

$$Q = \int_{V_{y^0}} M \cdot q dV_{y^0} \quad (2.23)$$

2.3 CZE/ABAQUS interface

The interface to ABAQUS is complicated (FORTRAN 77...) and is described in ABAQUS manuals. Aspects specific to the present implementation are discussed in this section.

2.3.1 Node and degree of freedom numbering

The CZ element is designed to be compatible with ABAQUS: looking from above, the nodes of the lower face are numbered in a counter-clockwise direction, followed by the nodes on the upper face (Figure 2.1).

In ABAQUS the degrees of freedom of each element are grouped by node. Further, the ABAQUS volume elements used jointly with the CZ are mechanical/heat diffusion elements, pressed to task with solute diffusion. Such elements use a lower order interpolation for heat diffusion, and only nodes at the vertices have temperature degrees of freedom.

For each node, the $n_x = 2$ or $n_x = 3$ displacement degrees of freedom come first. Then, if the node is a node with solute concentration degree of freedom, the degree of freedom for each solute is appended.

2.3.2 Limitations

In its present implementation, the CZE element can only handle non-linear static analysis. Dynamic analysis, in particular, are not supported, although returning a zero mass matrix will not be challenging.

In the present implementation, the Gauss schemes are hard coded for so-called exact integration. This could be made user-decidable using `jprop`.

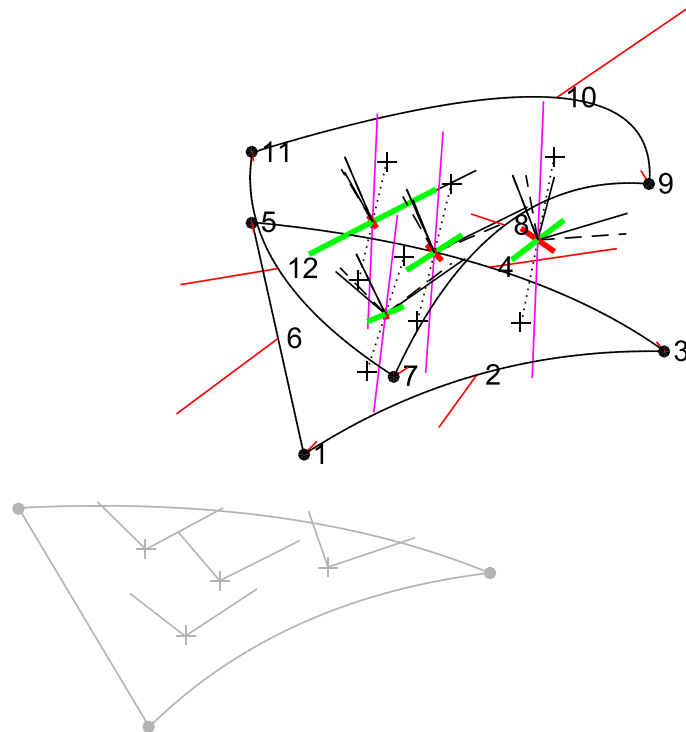


Figure 2.1: Node numbering in a linear-strain triangle cohesive zone element

In the present implementation, derivatives of duals (stiffness matrix etc.) is computed by finite differences. They should be computed from analytical derivatives if the TSL also provides analytical derivation.

2.4 TSL/CZE interface

The CZE provides the TSL at each Gauss point with `prop(2:)`, and with `jprop`. It also provides the TSL with a segment of `svar`, the state variables for both input and output.

Three “physical” inputs are provided, and correspondingly, their duals are taken as output (Table 1). `gapy`, `ty`, `epsy` and `sigy` are all expressed in the \mathbf{y} reference system.

name	intent	size	description	unit	
				3D	2D
<code>gapy</code>	in	(nx)	gap	[L]	
<code>ty</code>	out		traction	[L ⁻¹ T ⁻² M]	[T ⁻² M]
<code>epsy</code>	in	(nz,nz)	in-plane strain	[.]	
<code>sigy</code>	out		“membrane stress”	[T ⁻² M]	[LT ⁻² M]
<code>sgp</code>	in	$(nface \cdot ns)$	solute concentration	[molL ⁻³]	
<code>flow</code>	out		solute flow	[molL ⁻² T ⁻¹]	[molL ⁻¹ T ⁻¹]

Table 1: Input and output to the TSL

Note that the partial derivatives of the duals with respect to the primary variables are not part of the output: this is computed by the CZE using finite differences. This is intended to facilitate the exploration of different TSL.

3 DIFEL: element for diffusion and capture

3.1 Mechanics

3.1.1 Hypotheses

The volume within the element is modeled as a “continuum”. Depending on the scale of the model, a volume element may cover multiple grains, which are homogenized, or part of a grain.

In the current version, plasticity is not modeled, although everything is in place to add plasticity models, including plasticity models influenced by hydrogen concentration.

3.1.2 Equations

With these hypotheses, the equations to be solved are the classical equations of continuum mechanics. Equilibrium between the external volume forces (e.g. gravity) \bar{f} and the Cauchy stresses $\bar{\sigma}$ is written

$$\bar{\nabla} \cdot \bar{\sigma} = \bar{f} \quad (3.1)$$

where the Cauchy stress is expressed from the 2nd Piola-Kirchhoff (PK2) \bar{S} stresses

$$\bar{\sigma} = J^{-1} \bar{F} \cdot \bar{S} \cdot \bar{F}^T \quad (3.2)$$

where $J = \det \bar{F}$.

The PK2 stresses are related to the Green-Lagrange strain \bar{E} by the constitutive model,

$$\bar{S} = \bar{S}(\bar{E}) \quad (3.3)$$

(here simplified to the linear relation $\bar{S} = \bar{C} : \bar{E}$) and the Green-Lagrange strain is related to the deformation gradient \bar{F} by

$$\bar{E} = \frac{1}{2} \left(\bar{F}^T \cdot \bar{F} - \bar{I} \right) \quad (3.4)$$

3.1.3 Formulation

3.1.3.1 Deformation gradient

We introduce the shape function $\bar{N}^x(\bar{z})$ where \bar{X} are nodal positions, \bar{z} are the element's natural coordinates and $\bar{x}(\bar{z})$ are the coordinates of a material point within the element.

$$\bar{x}(\bar{z}) = \bar{N}^x(\bar{z}) \cdot \bar{X} \quad (3.5)$$

For brevity, the dependence on the natural coordinate \bar{z} is omitted from the notation in the following.

For an isoparametric formulation, with the convention that the derivative adds an index in front of the tensor, and sub-scripting with "0" variables related to the initial configuration,

$$\bar{F}^T \triangleq \frac{\partial \bar{x}}{\partial \bar{x}_0} \quad (3.6)$$

$$= \frac{\partial \bar{N}^x}{\partial \bar{x}_0} \cdot \bar{X} \quad (3.7)$$

$$= \bar{B}_0^x \cdot \Delta \bar{X} \quad (3.8)$$

with

$$\bar{\bar{\mathbf{B}}}_0^x \triangleq \frac{\partial \bar{\bar{\mathbf{N}}}^x}{\partial \bar{\mathbf{x}}_0} \quad (3.9)$$

$$= \left(\frac{\partial \bar{\mathbf{x}}_0}{\partial \bar{\mathbf{z}}} \right)^{-1} \cdot \frac{\partial \bar{\bar{\mathbf{N}}}^x}{\partial \bar{\mathbf{z}}} \quad (3.10)$$

$$= \left(\frac{\partial \bar{\bar{\mathbf{N}}}^x}{\partial \bar{\mathbf{z}}} \cdot \bar{\mathbf{x}}_0 \right)^{-1} \cdot \frac{\partial \bar{\bar{\mathbf{N}}}^x}{\partial \bar{\mathbf{z}}} \quad (3.11)$$

3.1.3.2 Isoparametric element

An isoparametric formulation provides good flexibility when creating meshes. Introducing

$$\bar{\bar{\mathbf{B}}}^x \triangleq \frac{\partial \bar{\bar{\mathbf{N}}}^x}{\partial \bar{\mathbf{x}}} \quad (3.12)$$

$$= \frac{\partial \bar{\mathbf{x}}_0}{\partial \bar{\mathbf{x}}} \cdot \frac{\partial \bar{\bar{\mathbf{N}}}^x}{\partial \bar{\mathbf{x}}_0} \quad (3.13)$$

$$= \bar{\bar{\mathbf{F}}}^{-T} \cdot \bar{\bar{\mathbf{B}}}_0^x \quad (3.14)$$

and writing the weak form of the equilibrium equation 3.1 (with an integral in the instant configuration), and carrying out a partial integration yields

$$\bar{\mathbf{R}}^x = \int_{\mathbf{v}} \bar{\bar{\mathbf{B}}}^{xT} : \bar{\bar{\boldsymbol{\sigma}}} \, d\mathbf{v} + \int_{\mathbf{v}} \bar{\bar{\mathbf{N}}}^x \cdot \bar{\mathbf{f}} \, d\mathbf{v} \quad (3.15)$$

$$= \int_{\mathbf{V}} \bar{\bar{\mathbf{B}}}^{xT} : \bar{\bar{\boldsymbol{\sigma}}} J \, d\mathbf{V} + \int_{\mathbf{V}} \bar{\bar{\mathbf{N}}}^x \cdot \bar{\mathbf{f}} J \, d\mathbf{V} \quad (3.16)$$

$$= \int_{\mathbf{V}} \bar{\bar{\mathbf{B}}}_0^{xT} : \left(\bar{\bar{\mathbf{F}}}^{-1} \cdot \bar{\bar{\boldsymbol{\sigma}}} \right) J \, d\mathbf{V} + \int_{\mathbf{V}} \bar{\bar{\mathbf{N}}}^x \cdot \bar{\mathbf{f}} J \, d\mathbf{V} \quad (3.17)$$

$$= \int_{\mathbf{V}} \bar{\bar{\mathbf{B}}}_0^{xT} : \left(\bar{\bar{\mathbf{S}}} \cdot \bar{\bar{\mathbf{F}}}^T \right) \, d\mathbf{V} + \int_{\mathbf{V}} \bar{\bar{\mathbf{N}}}^x \cdot \bar{\mathbf{f}} J \, d\mathbf{V} \quad (3.18)$$

where $\bar{\bar{\mathbf{S}}} \cdot \bar{\bar{\mathbf{F}}}^T$ is known as the nominal stress. Letting the material model return the PK2 nominal stress makes it unnecessary to inverse $\bar{\bar{\mathbf{F}}}$.

3.1.3.3 Mixed element

It is important to provide good quality gradients of the triaxial pressure, since pressure gradients are one of the drivers of hydrogen diffusion.

Triaxial pressure is notoriously difficult to compute in displacement-based elements, which are prone to volumetric locking. Pressure gradients are even more difficult to

obtain with these elements. To get the require quality of pressure gradient, a mixed formulation is used. Several such formulations exist ([1][5]). In the present work, the pressure \mathbf{p} and the dilatation (the triaxial part of strain) \mathbf{d} are interpolated separately [7, 6] :

$$\mathbf{d}(\bar{\mathbf{z}}) = \bar{\mathbf{N}}^{\mathbf{d}}(\bar{\mathbf{z}}) \cdot \bar{\mathbf{D}} \quad (3.19)$$

$$\mathbf{p}(\bar{\mathbf{z}}) = \bar{\mathbf{N}}^{\mathbf{p}}(\bar{\mathbf{z}}) \cdot \bar{\mathbf{P}} \quad (3.20)$$

where the dependence on the natural coordinate $\bar{\mathbf{z}}$ will be kept implicit in the following.

The deviator operator can be written as

$$\text{dev}_{ijkl} = \delta_{ik}\delta_{jl} - n_x^{-1}\delta_{ij}\delta_{kl} \quad (3.21)$$

To ensure stability of the numerical scheme, $\bar{\mathbf{N}}^{\mathbf{d}}$ and $\bar{\mathbf{N}}^{\mathbf{p}}$ must be chosen of lower order than $\bar{\mathbf{N}}^{\mathbf{x}}$ [2, 3, 4].

The residuals can be written

$$\bar{\mathbf{R}}^{\mathbf{x}} = \int_V \bar{\bar{\mathbf{B}}}^{\mathbf{xT}} : \bar{\bar{\boldsymbol{\sigma}}} (1 + \mathbf{d}) dV + \int_V \bar{\bar{\mathbf{N}}}^{\mathbf{xT}} \cdot \bar{\mathbf{f}} J dV \quad (3.22)$$

$$\bar{\mathbf{R}}^{\mathbf{d}} = \int_V \bar{\mathbf{N}}^{\mathbf{d}} \left(n_x^{-1} \bar{\bar{\mathbf{I}}} : \bar{\bar{\boldsymbol{\sigma}}}^* - \mathbf{p} \right) dV \quad (3.23)$$

$$\bar{\mathbf{R}}^{\mathbf{p}} = \int_V \bar{\mathbf{N}}^{\mathbf{p}} \left(\det \bar{\bar{\mathbf{F}}} - (1 + \mathbf{d}) \right) dV \quad (3.24)$$

(remembering that the force is $-\bar{\mathbf{R}}^{\mathbf{x}}$) with

$$J = \det \bar{\bar{\mathbf{F}}} \quad (3.25)$$

$$\theta = \left(\frac{1 + \mathbf{d}}{J} \right)^{n_x^{-1}} \quad (3.26)$$

$$\bar{\bar{\mathbf{F}}}^* = \theta \bar{\bar{\mathbf{F}}} \quad (3.27)$$

$$\bar{\bar{\boldsymbol{\sigma}}}^* = \bar{\bar{\mathcal{M}}}(\bar{\bar{\mathbf{F}}}^*) \quad (3.28)$$

$$\bar{\bar{\boldsymbol{\sigma}}} = \text{dev} \bar{\bar{\boldsymbol{\sigma}}}^* + \bar{\bar{\mathbf{I}}} \theta^{-n_x} \mathbf{p} \quad (3.29)$$

Note that because of the way the Cauchy stress is computed in 3.29, it is not possible to adapt 3.18, instead 3.22 is adapted from 3.16: in the hybrid formulation, $\bar{\bar{\mathbf{F}}}$ must be inverted.

3.1.4 Plasticity

Both a linear elastic and a elastoplastic model are implemented. For the elastoplastic model, the hardening law is of the form

$$\boldsymbol{\sigma}_y(\varepsilon_{peq}) = \mathbf{p}_1 + \mathbf{p}_2 \varepsilon_{peq}^{\mathbf{p}_3} \quad (3.30)$$

Currently, the input system does not allow to switch the elastoplastic model on.

3.2 Heat diffusion

The conservation of energy is written as

$$\dot{h} + \frac{\partial}{\partial \bar{x}_0} \cdot \bar{\phi}^h = \dot{w}^h \quad (3.31)$$

where the heat generation \dot{w}^h is a function of plastic work, compression, mass diffusion and trapping-untrapping. All quantities are here referred to the undeformed configuration: densities are per unit original volume, flow is per unit original surface, gradient is with respect to material coordinates.

To set ideas, a typical model is

$$\dot{h} = \rho_0 c^t \dot{T} \quad (3.32)$$

and

$$\bar{\phi}^h = D^t \frac{\partial}{\partial \bar{x}_0} T \quad (3.33)$$

but the equation is more generally applicable.

The weak form of this equation is

$$0 = \int_V \delta T \left(\dot{h} + \frac{\partial}{\partial \bar{x}_0} \cdot \bar{\phi}^h - \dot{w}^h \right) dV \quad (3.34)$$

$$= \int_V \delta T (\dot{h} - \dot{w}^h) dV + \int_V \delta T \cdot \frac{\partial}{\partial \bar{x}_0} \cdot \bar{\phi}^h dV \quad (3.35)$$

$$= \int_V \delta T (\dot{h} - \dot{w}^h) dV - \int_V \frac{\partial}{\partial \bar{x}_0} \delta T \cdot \bar{\phi}^h dV + \int_S \delta T \bar{\phi}^h \cdot d\bar{S} \quad (3.36)$$

Introducing the discretization

$$T = \bar{N}^t \cdot \bar{T} \quad (3.37)$$

$$\frac{\partial}{\partial \bar{x}_0} T = \bar{B}^t \cdot \bar{T} \quad (3.38)$$

(note the material derivative, as opposed to $\frac{\partial}{\partial \bar{x}}$) the weak form becomes

$$\bar{R}^t = \int_V \bar{N}^t (\dot{h} - \dot{w}^h) dV - \int_V \bar{B}^{tT} \cdot \bar{\phi}^h dV + \int_S \bar{N}^t \phi ds \quad (3.39)$$

3.3 Mass diffusion and trapping

3.3.1 Trapping

3.3.1.1 Working with kinetics

Kinetic models can describing both “fast” and “slow” reactions. By contrast, a model of thermodynamic equilibrium can only accommodate fast reactions. As a consequence, a system based on reaction kinetics is more flexible. In particular, the

untrapping of hydrogen (in the presence of a decreased lattice concentration, or an increase of temperature) will slow.

In the following, trapping and untrapping are termed “reactions”, as they are a special case with a one to one reaction between lattice and trapped hydrogen. In the presence of multiple types of trapping sites, we have a special case of “chemical reaction network”.

One concern about using reaction kinetics, is that one may want to use time steps in the analysis, which are longer than the time it takes for some fast reaction to converge to thermodynamic equilibrium. In many settings, long numeric step times compared to physical time scales are a source of numerical instability. However, as long as the complete model only has first order time derivatives (not accounting for structural dynamics, in particular), it is possible to use the backward Euler method for time integration. This method is unconditionally stable (stable for any time step size): for fast reactions, the solution evolves towards thermodynamic equilibrium in 2 or 3 time steps. Of course the rate of evolution is wrong, but if one is prepared to disregard this, the results are perfectly usable.

Another concern is that experimentally determining the parameters of kinetic laws may be impracticable in some cases, and in all cases, more work than describing thermodynamic equilibrium. This is true in particular for fast reactions. Luckily, in such cases, the kinetic model does not have to be accurate, it only needs to imply the correct equilibrium. For example in transition state theory, the difference in Gibbs energy between the left hand side and the right hand side of an equation, can be established, while the Gibbs energy of the transition state is harder to estimate. This energy can however be set arbitrarily to a small fraction of the difference in Gibbs energy between left and right: this ensures fast kinetics, and the proper equilibrium.

The stability of the numerical solution is achieved by choosing an implicit Euler time integration scheme, which is of the first order, and unconditionally stable.

3.3.1.2 Chemical reaction network

The r th reaction r is noted as



where the positive integers v_{ri}^- and v_{ri}^+ are the stoichiometric coefficients of the i -th species. In this equation, s_i is the i th species, not its concentration.

The rate of production (or consumption if negative) u_{ir} of a species s_i in reaction r is

$$u_{ir} = \xi_r (v_{ri}^+ - v_{ri}^-) \quad (3.41)$$

$$= \xi_r v_{ri} \quad (3.42)$$

with

$$\mathbf{v}_{ri} \equiv \mathbf{v}_{ri}^+ - \mathbf{v}_{ri}^- \quad (3.43)$$

where ξ_r is the reaction rate. The above models chemistry as a “chemical reaction network”. Closures to the model are needed in the form of kinetic models, giving the reaction rate as a function of temperature and reactant concentrations. Examples of kinetic models are presented in the following.

3.3.1.3 State transition reactions

The case of interest here is the transition between hydrogen at one energy level (s_i) and another (s_j). We then have $\mathbf{v}_{rk}^- = \delta_{ik}$ and $\mathbf{v}_{rk}^+ = \delta_{jk}$.

In this case, the kinetic of the reaction is

$$\xi_r = s_i \mathcal{K}_{ij} \frac{n_j - s_j}{n_j} \frac{n_j}{\sum_k n_k} - s_j \mathcal{K}_{ji} \frac{n_i - s_i}{n_i} \frac{n_i}{\sum_k n_k} \quad (3.44)$$

$$= s_i \frac{n_j - s_j}{\sum_k n_k} \mathcal{K}_{ij} - s_j \frac{n_i - s_i}{\sum_k n_k} \mathcal{K}_{ji} \quad (3.45)$$

where

$$\mathcal{K}_{ij} = \omega(T) \exp\left(-\frac{G_{ij}}{RT}\right) \quad (3.46)$$

G_{ij} is the *activation energy* from energy level i to j . T is the absolute temperature. R is the perfect gas constant.

3.3.1.4 “Many lattice site” approximation

The number of lattice sites n_i is much larger than the concentration of hydrogen in the lattice, and than the number of sites at other energy levels: $\frac{n_i - s_i}{n_i} \frac{n_i}{\sum_k n_k} \approx 1$. Further, $A_{ij}(T) = \omega(T) \frac{n_j}{\sum_k n_k}$ denotes the frequency with which a molecule is positioned at the vicinity of an adsorption site

$$\xi_r = s_i \mathcal{K}_{ij} \frac{n_j - s_j}{n_j} \frac{n_j}{\sum_k n_k} - s_j \mathcal{K}_{ji} \frac{n_i - s_i}{n_i} \frac{n_i}{\sum_k n_k} \quad (3.47)$$

$$= s_i \frac{n_j - s_j}{n_j} A_{ij}(T) \exp\left(-\frac{G_{ij}}{RT}\right) - s_j \omega(T) \exp\left(-\frac{G_{ji}}{RT}\right) \quad (3.48)$$

Since temperature is a mean kinetic energy, mean velocity will be proportional to \sqrt{T} so that

$$\xi_r = s_i \frac{n_j - s_j}{n_j} a_{ij} \sqrt{T} \exp\left(-\frac{G_{ij}}{RT}\right) - s_j \omega \exp\left(-\frac{G_{ji}}{RT}\right) \quad (3.49)$$

3.3.1.5 Law of mass action

The above is a special case of the law of mass action, which can be written as

$$\xi_r = K^+ \prod_i s_i^{m_{ri}^-} - K^- \prod_i s_i^{m_{ri}^+} \quad (3.50)$$

with

$$K^+ = \omega(T) \exp\left(-\frac{\Delta G_r^+}{RT}\right) \quad (3.51)$$

$$K^- = \omega(T) \exp\left(-\frac{\Delta G_r^-}{RT}\right) \quad (3.52)$$

3.3.1.6 General purpose model

A model that covers a range of possible reaction is proposed, to give flexibility in further software development: The equations

$$\omega^+ = a^+ T^{e^+} \quad (3.53)$$

$$K^+ = \exp\left(-\frac{\Delta G_r^+}{RT}\right) \quad (3.54)$$

$$p^+ = \prod_i s_i^{m_{ri}^+} \quad (3.55)$$

$$q^+ = \prod_i \left(\frac{n_i - s_i}{n_i}\right)^{m_{ri}^-} \quad (3.56)$$

$$\xi_r^+ = \omega^+ K^+ p^+ q^+ \quad (3.57)$$

represent the kinetic of the forward reaction, and model of the backward reaction has the same form. Note that m_{ri}^- (minus) appears in the expression for q^+ (plus). By careful choice of the parameters a^+ , e^+ and n_i^+ , (and correspondingly for the backward equation) all the above models can be accommodated. The user can be spared the work of choosing these coefficients, by means of computer code (know as “constructors”) that will translate physics-related parameters into the parameters of this general model.

3.3.1.7 Improving convergence

Concentrations are constrained into the domain $\forall i \in \{1..n\} 0 < s_i < n_i$. Outside of this domain, equations like 3.55 or 3.56 have “strange” behavior. The Newton iteration process is not restricted to exploring values within the physical range.

Hence to ensure converges, it is necessary to extend the above equation outside of the physical range, to avoid convergence problems.

If we have n species involved in the reaction, the above-mentioned domain is a rectangle parallelepiped with 2^n vertices: for 2 species the domain is a square (2^2 vertices), for 3 species, a cube (2^3 vertices) and so forth.

A vertex ν can be addressed by a set of values w_i^ν : for each species i , $w_i^\nu = 0$ if the vertex corresponds to $s_i = 0$, and $w_i^\nu = 1$ if the vertex corresponds to $s_i = n_i$. We introduced the change of variable

$$s_i^* = s_i \quad \text{where } w_i^\nu = 0 \quad (3.58)$$

$$s_i^* = n_i - s_i \quad \text{where } w_i^\nu = 1 \quad (3.59)$$

This change of variables ensures that the vertex has coordinates $s_i^* = 0$ and all $s_i^* > 0$ in the domain.

In the general purpose model, the reaction rate is a polynomial P in the concentrations s_i . One can express this polynomial in term of s_i^* concentrations, and expand the polynomial. Then, in all monomials of total order strictly higher than 1, all variables s_i^* are replaced by $\langle s_i^* \rangle \triangleq \max(0, s_i^*)$. The expression is then transformed back $s_i^* \rightarrow s_i$. This results for each vertex ν in a function $f^\nu(s_i \quad i \in 1..n)$ which

1. Is identical to the original polynomial in the domain.
2. Is C_0 everywhere.
3. Is C_1 at the vertex, and at all the edges passing through this vertex.

In order to construct a function ξ^* that is C_1 everywhere, the 2^n functions f^ν are merged. We introduce a sigmoid function σ

$$\sigma(x) = 0 \quad \text{for } x < 0 \quad (3.60)$$

$$\sigma(x) = -2x^3 + 3x^2 \quad \text{for } 0 < x < 1 \quad (3.61)$$

$$\sigma(x) = 1 \quad \text{for } 1 < x \quad (3.62)$$

which is C_1 everywhere and always verifies

$$\sigma(x) + \sigma(1-x) = 1 \quad (3.63)$$

We introduce

$$\sigma^\nu(s_i \quad i \in 1..n) = \prod_{w_i^\nu=0} \sigma\left(\frac{s_i}{n_i}\right) \prod_{w_i^\nu=1} \sigma\left(1 - \frac{s_i}{n_i}\right) \quad (3.64)$$

which is equal to 1 at vertex ν and 0 at all other vertices. The modified model is then defined as

$$\xi_r^{+*}(s_i \quad i \in 1..n) \triangleq \sum_{\nu} \sigma^\nu(s_i \quad i \in 1..n) f^\nu(s_i \quad i \in 1..n) \quad (3.65)$$

Figure 3.1 provides an example of such a construction. The left graph shows the original polynomial with roots (thermodynamic equilibrium) outside of the domain, found to cause instability. The left graph is obtained by the present procedure.

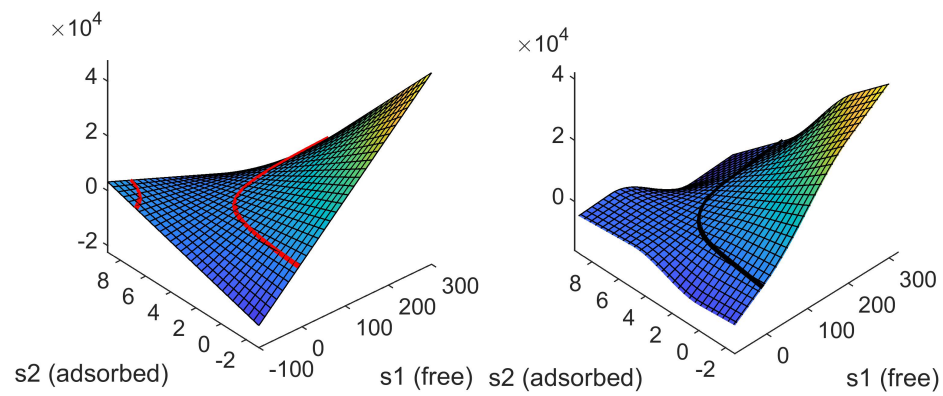


Figure 3.1: Reaction rate as a function of the concentrations of free and adsorbed chloride. Original formulation (left) and correct formulation (right)

3.3.2 Diffusion and conservation

The concentration of species i is noted s_i . The conservation of mass is given as

$$\forall i \quad \dot{s}_i - \sum_r \xi_r \nu_{ri} + \frac{\partial}{\partial \bar{x}^0} \cdot \bar{\Phi}_i(\bar{\nabla} s_i, s_i, \bar{\varepsilon}, \bar{\nabla} p) = 0 \quad (3.66)$$

As for the heat diffusion, all quantities are here referred to the undeformed configuration: density are per unit original volume, flow is per unit original surface, gradient is with respect to material coordinates.

To set ideas, the mass flow may be modeled as

$$\bar{\Phi}_i = -\bar{D}_i^s \cdot \frac{\partial}{\partial \bar{x}^0} s_i + \bar{D}_i^p \cdot \frac{\partial}{\partial \bar{x}^0} p s_i \quad (3.67)$$

where p is the *opposite* of the pressure, but the element formulation is more general.

3.3.3 Weak form

The weak form of the differential equation is obtained by requiring that for any "virtual variation" δc_i of the unknown field c_i , equation (3.66) multiplied by δc_i and integrated over the reference domain V , must be verified

$$\forall i \quad 0 = \int_V \delta s_i \dot{s}_i dV + \int_V \delta s_i g_i dV + \int_V \delta s_i \frac{\partial}{\partial \bar{x}^0} \cdot \bar{\Phi}_i dV \quad (3.68)$$

$$= \int_V \delta s_i \dot{s}_i dV + \int_V \delta s_i g_i dV + \int_V \frac{\partial}{\partial \bar{x}^0} \cdot (\delta s_i \bar{\Phi}_i) dV - \int_V \frac{\partial}{\partial \bar{x}^0} \delta s_i \cdot \bar{\Phi}_i dV \quad (3.69)$$

$$= \int_V \delta s_i \dot{s}_i dV + \int_V \delta s_i g_i dV + \int_S \bar{n} \cdot \delta s_i \bar{\Phi}_i dS - \int_V \frac{\partial}{\partial \bar{x}^0} \delta s_i \cdot \bar{\Phi}_i dV \quad (3.70)$$

$$= \int_V \delta s_i \dot{s}_i dV + \int_V \delta s_i g_i dV + \int_S \delta s_i \phi_i dS - \int_V \frac{\partial}{\partial \bar{x}^0} \delta s_i \cdot \bar{\Phi}_i dV \quad (3.71)$$

with

$$\phi_i = \bar{n} \cdot \bar{\Phi}_i \quad (3.72)$$

where \bar{n} is the outward-pointing normal to the surface s and ϕ_i is the flow of solute i through the surface s .

$$g_i = - \sum_r \xi_r \nu_{ri} \quad (3.73)$$

is the rate of production of species i by all reactions. Again, \dot{s}_i and g_i are densities related to the original volume.

The integration by parts has allowed to introduce boundary conditions: at any point of the surface s , either ϕ_i must be known (non-essential boundary condition) or δs_i must be zero (essential boundary condition).

We introduce the interpolation

$$s_i = \bar{N}^s \cdot \bar{S}_i \quad (3.74)$$

$$\frac{\partial}{\partial \bar{x}_0} s_i = \bar{\bar{B}}^s \cdot \bar{S}_i \quad (3.75)$$

with

$$\bar{\bar{B}}^s \triangleq \frac{\partial \bar{N}^s}{\partial \bar{x}_0} \quad (3.76)$$

$$= \left(\frac{\partial \bar{x}_0}{\partial \bar{z}} \right)^{-1} \cdot \frac{\partial \bar{N}^s}{\partial \bar{z}} \quad (3.77)$$

$$= \left(\frac{\partial \bar{N}^x}{\partial \bar{z}} \cdot \bar{X}_0 \right)^{-1} \cdot \frac{\partial \bar{N}^s}{\partial \bar{z}} \quad (3.78)$$

Similarly

$$p = \bar{N}^p \cdot \bar{P} \quad (3.79)$$

$$\bar{\nabla} p = \bar{\bar{B}}^p \cdot \bar{P} \quad (3.80)$$

with

$$\bar{\bar{B}}^p \triangleq \left(\frac{\partial \bar{N}^x}{\partial \bar{z}} \cdot \bar{X}^0 \right)^{-1} \cdot \frac{\partial \bar{N}^p}{\partial \bar{z}} \quad (3.81)$$

Posing

$$\delta s_i = \bar{N}^s \cdot \delta \bar{S}_i \quad (3.82)$$

and requesting that (3.71) be verified for any $\delta \bar{S}_i$ leads to $\bar{R}_i^s = \bar{0}$ with

$$\forall i \quad \bar{R}_i^s \triangleq \int_V \bar{N}^s (\dot{s}_i + f_i) dV - \int_V \bar{\bar{B}}^{sT} \cdot \bar{\Phi}_i dV + \int_s \bar{N}^s \phi_i ds \quad (3.83)$$

4 User manual

The present text assumes that the reader is familiar with ABAQUS *.inp files and has access to the ABAQUS manual. A sample file is provided in Section A. Line numbers mentioned in the following text refer to the line numbers in the appendix.

Line 12: All input in this file *must* be in SI base unit (m, s, kg, mol).

Line 33 describes a “user defined” DIFEL element. Although the code of the user defined element is connected to ABAQUS, ABAQUS knows nothing about it. The DIFEL elements that have been defined are described in Table DIFEL element types.

Lines 35 to 42 tell ABAQUS which types of degrees of freedom each node of the element has. The fragments below must be copied verbatim, including the missing node number on the first line. For U101:

TYPE	Description	NODES	COORDINATES	PROPERTIES	IPROPERTIES	VAR
U101	Fully integrated tri-quadratic hexahedron	20	3	14	4	54
U102	Fully integrated quadratic triangle	6	2	14	4	6
U103	Fully integrated bi-quadratic rectangle	8	2	14	4	18

Table 2: DIFEL element types

1, 2, 3, 12, 13,7, 8
 2, 1, 2, 3, 12, 13,7, 8
 3, 1, 2, 3, 12, 13,7, 8
 4, 1, 2, 3, 12, 13,7, 8
 5, 1, 2, 3, 12, 13,7, 8
 6, 1, 2, 3, 12, 13,7, 8
 7, 1, 2, 3, 12, 13,7, 8
 8, 1, 2, 3, 12, 13,7, 8
 9, 1, 2, 3
 10, 1, 2, 3
 11, 1, 2, 3
 12, 1, 2, 3
 13, 1, 2, 3
 14, 1, 2, 3
 15, 1, 2, 3
 16, 1, 2, 3
 17, 1, 2, 3
 18, 1, 2, 3
 19, 1, 2, 3
 20, 1, 2, 3

For U102

1, 2,12, 13,7, 8
 2, 1, 2,12, 13,7, 8
 3, 1, 2,12, 13,7, 8
 4, 1, 2,12, 13,7, 8
 5, 1, 2
 6, 1, 2
 7, 1, 2
 8, 1, 2

For U103

1, 2,12, 13,7, 8
 2, 1, 2,12, 13,7, 8
 3, 1, 2,12, 13,7, 8
 4, 1, 2
 5, 1, 2
 6, 1, 2

TYPE	Description	NODES	COORDINATES	PROPERTIES	IProperties	VAR
U1	Fully integrated bi-linear rectangle	8	3	5*	2	1
U2	Over integrated bi-quadratic rectangle	16	3	5*	2	1
U3	Fully integrated quadratic line	6	2	5*	2	1

Table 3: CZE element types

Line 44 is standard ABAQUS input, and the element type must correspond to a type defined as described above.

Line 48 describes a “user defined” CZE element. The CZE elements that have been defined are described in Table CZE element types. The actual value of PROPERTIES depends on the TSL chosen.

Lines 35 to 42 tell ABAQUS which types of degrees of freedom each node of the element has. The fragments below must be copied verbatim, including the missing node number on the first line. For U1:

```

      1, 2, 7, 8
2,    1, 2, 7, 8
3,    1, 2, 7, 8
4,    1, 2, 7, 8
5,    1, 2, 7, 8
6,    1, 2, 7, 8
7,    1, 2, 7, 8
8,    1, 2, 7, 8

```

For U2

```

      1, 2, 7, 8
2,    1, 2
3,    1, 2, 7, 8
4,    1, 2
5,    1, 2, 7, 8
6,    1, 2
7,    1, 2, 7, 8
8,    1, 2
9,    1, 2, 7, 8
10,   1, 2
11,   1, 2, 7, 8
12,   1, 2
13,   1, 2, 7, 8
14,   1, 2
15,   1, 2, 7, 8
16,   1, 2

```

For U3

```

      1, 2, 7, 8
2,    1, 2

```

Name	Description	Typical	Unit
visc	viscosity coefficient	0.	Ns m^{-3}
δ_c	critical separation	10^{-4}	m
σ_{c0}	critical stress w/o H	10^8	Pa
C_0	critical concentration	10^3	$\text{mol} \cdot \text{m}^{-3}$
k	shear stiffness	10^{10}	Pa
ns	number of hydrogen levels	2	Integer
mat	selection of TSL	4	Integer

Table 4: Material parameters for CZE elements, assuming mat=4

3, 1, 2, 7, 8

4, 1, 2, 7, 8

5, 1, 2

6, 1, 2, 7, 8

Lines 62, 63 and 65, 66 specify “element sets” needed to associate properties (in particular material properties) to the elements.

Lines 70, 71 associate properties to the set containing the unique CZE element. The description provided in Table Material parameters for CZE elements, assuming mat=4 is for the Needleman TSL model.

Lines 76 to 79 associate properties to the set containing the DIFEL elements. The description is provided in Table Material parameters for CZE elements.

Lines 110 to 120. ABAQUS must have at least one material definition in a file – even though here, this data is dummy.

Line 125: step specification. The option UNSYMM=YES might not be needed, but this has not been tested.

Line 126: ABAQUS’ “soils consolidation” solution algorithm must be used, as it provides an implicit-Euler time integration together with a linear equation solver tackling asymmetric indefinite systems.

A Sample *.inp file

The following is an ABAQUS *.inp file, which describes a “sandwich test”: a square CZE element with a cubic DIFEL element on each side.

```

1 *HEADING
2 *PREPRINT, ECHO = NO, MODEL = NO, HISTORY = NO, CONTACT = NO
3 **
4 ** 2D Sandwich test with DIFEL and CZE
5 **
6 *PART, NAME = Part-1
7 **
8 *****

```

Name	Description	Typical	Unit
T	Temperature	293.	K
E	Young's modulus	$2.1 \cdot 10^{11}$	Pa
ν	Poisson coefficient	0.3	.
p1	plasticity 1	$4 \cdot 10^8$	Pa
p2	plasticity 2	10^9	Pa
p3	plasticity 3	0.5	.
ρ_r	mass density	8000	$\text{kg} \cdot \text{m}^{-3}$
c_t	specific heat	447.	$\text{J} \cdot \text{kg}^{-1} \cdot \text{K}^{-1}$
D_t	thermal conductivity	80.4	$\text{W}/(\text{K}/\text{m})/(\text{kg}/\text{m}^3)$
D_s	mass diffusivity		$\text{m}^2 \cdot \text{s}^{-1}$
G	Trapping energy	10^4	$\text{J} \cdot \text{mol}^{-1}$
n_{site}	Trap density	0.3	$\text{mol} \cdot \text{m}^{-3}$
f	Attempt frequency	100	s^{-1}
R	The gas constant	8.31	$\text{J} \cdot \text{mol}^{-1} \cdot \text{K}^{-1}$
ns	Number of hydrogen levels	2	Integer
nt	Switch for temperature	0	Integer
npd	0: disp-based, 1:hybrid	1	Integer
mattyp	1: concrete, 2:metal	2	Integer

Table 5: Material parameters for CZE elements

```

9  **
10 **Nodes coordinates
11 **node number, node x-coordinate, node y-coordinate, node z-
    coordinate
12 **Values are in S.I. units (i.e. m)
13 ** *NODE
14 1, .00, .00
15 2, .02, .00
16 3, .02, .02
17 4, .00, .02
18 5, .01, .00
19 6, .02, .01
20 7, .01, .02
21 8, .00, .01
22 9, .00, -.02
23 10, .02, -.02
24 11, .02, .00
25 12, .00, .00
26 13, .01, -.02
27 14, .02, -.01
28 15, .01, .00
29 16, .00, -.01
30 **
31 ****
32 ** DIFEL

```

```

33 *USER ELEMENT, TYPE = U103, NODES = 8, COORDINATES = 2, PROPERTIES
    = 14, IPROPERTIES = 4, VAR = 54
34 **  x1 x2 p  d  s1 s2
35      1, 2,12, 13,7, 8
36 2,      1, 2,12, 13,7, 8
37 3,      1, 2,12, 13,7, 8
38 4,      1, 2,12, 13,7, 8
39 5,      1, 2
40 6,      1, 2
41 7,      1, 2
42 8,      1, 2
43 **
44 *ELEMENT, TYPE = U103
45 1, 1,2,3,4,5,6,7,8
46 2, 9,10,11,12,13,14,15,16
47 **
48 *USER ELEMENT, TYPE = U3, NODES = 6, COORDINATES = 2, PROPERTIES =
    5, IPROPERTIES = 2, VAR = 1
49 **  x1 x2 s1 s2
50      1, 2, 7, 8
51 2, 1, 2
52 3, 1, 2, 7, 8
53 4, 1, 2, 7, 8
54 5, 1, 2
55 6, 1, 2, 7, 8
56 **
57 *ELEMENT, TYPE = U3
58 3, 12,15,11,1,5,2
59 **
60 *****
61 **
62 *ELSET, ELSET = czeElSet
63 3
64 **
65 *ELSET, ELSET = difeElSet, GENERATE
66 1, 2
67 **
68 *****
69 ** visc delta_c sigma_c0 C0      k      ns mat
70 *UEL PROPERTY, ELSET = czeElSet
71 0., 1e-3, 1.e8, 1.e3, 1.e10, 2, 4
72 *****
73 ** T E      v      p1      p2      p3      rhor ct
74 ** Dt Ds Gibbs nsite attempt R      ns nt
75 ** npd mattyp
76 *UEL PROPERTY, ELSET = difeElSet
77 293., 2.1e11, 0.3, 4.e8, 1.e9, .5, 8000., 447.
78 80.4, 1., 1.e4, 0.3, 1.e2, 8.31, 2, 0
79 1,2
80 *END PART
81 *****

```

```

82 **
83 *ASSEMBLY, NAME = Assembly
84 **
85 *****
86 **
87 *INSTANCE, NAME = Part-1-1, PART = Part-1
88 *END INSTANCE
89 **
90 *****
91 **
92 **Some node sets usefull to apply boundary conditions (not all of
93 ** them are needed for the current alalysis)
94 **
95 *NSET, NSET = TopBoundary, INSTANCE = Part-1-1 4,7,3
96 *NSET, NSET = BottomBoundary, INSTANCE = Part-1-1 9,13,10
97 *NSET, NSET = LeftBoundary, INSTANCE = Part-1-1 4,8,1,12,16,9
98 *NSET, NSET = AllNodes, INSTANCE = Part-1-1, GENERATE 1, 16, 1
99 *END ASSEMBLY
100 *****
101 **
102 ** MODEL DATA BOUNDARY CONDITIONS
103 **
104 **Are defined before a
105 *STEP
106 *BOUNDARY
107 *****
108 **
109 ** DUMMY - not used by UEL, but necessary to apease ABAQUS
110 *MATERIAL, name = Material-1
111 *CONDUCTIVITY
112 50.,
113 *DENSITY
114 7.8e-06,
115 *ELASTIC
116 210000., 0.3
117 *SPECIFIC HEAT
118 1.,
119 *PERMEABILITY, SPECIFIC = 1.
120 1., .1, 0.
121 *****
122 **
123 ** STEP: Step-Temp
124 **
125 *STEP, NAME = Step-Temp, NLGEOM = YES, AMPLITUDE = RAMP, INC = 100,
    UNSYMM = YES
126 *SOILS, CONSOLIDATION, HEAT = NO 0.1, 1., 1e-4, 0.1
127 **
128 ** HISTORY DATA BOUNDARY CONDITIONS
129 **
130 ** NOTE: Specifing only the first DOF where the BC applies doesn't
    work

```

```
131 ** although the documentation states otherwise
132 **
133 *BOUNDARY
134 AllNodes,          3 , 3, 0.0
135 TopBoundary,      2 , 2, 0.001
136 BottomBoundary,  2 , 2, 0.0
137 LeftBoundary,     1 , 1, 0.0
138 ***** REMEMBER SCALING *****
139 TopBoundary,      7, 7, 0.1
140 BottomBoundary,  7, 7, 0.1
141 *****
142 *OUTPUT, FIELD, VARIABLE = PRESELECT
143 *OUTPUT, HISTORY, VARIABLE = PRESELECT
144 *END STEP
```


References

- [1] D. Al Akhrass, S. Drapier, J. Bruchon, and S. Fayolle. Stabilized finite element method to deal with incompressibility in solid mechanics in finite strains. In *European congress on computational methods*, 2012.
- [2] I. Babuska. Error bounds for finite element method. *Numerische Mathematik*, 16:322–333, 1971.
- [3] F. Brezzi. On the existence, uniqueness and approximation of saddle-point problems arising from lagrange multipliers. *R.A.I.R.O.*, 8, R2:129–151, 1974.
- [4] Franco Brezzi and Donatella Marini. Subgrid phenomena and numerical schemes.
- [5] D. Chappelle and K. J. Bathe. The inf-sip test. *Computers and structures*, 47(4/5):537–545, 1993.
- [6] Kjell Magne Mathisen, Knut Moten Olstad, Trond Kvamsdal, and Siv Bente Rønes. Isogeometric analysis of finite deformation nearly incompressible solids. *Rakenteiden Mekaniikka*, 44(3):pp. 260 – 278, 2011.
- [7] J.C. Simo, R.L. Taylor, and K.S. Pister. Variational and projection methods for the volume constraint in finite deformation in elasto-plasticity. *Computer methods in applied mechanics and engineering*, 51:pp. 177 – 208, 1985.